

The influence of shear stress on Human Mammary Fibroblast to induce CAF-like characteristics

Jelle Mört (s2387042) BMT-student

Daily & main supervisor: dr. ir. Kirsten Pondman

Chair of committee: prof. dr. ir. Séverine Le Gac

External member of committee: prof. dr. Robert Passier

AMBER - University of Twente

7/3/2024

Abstract

In blood of patients with metastatic breast cancer, Circulating Tumor Cells (CTCs) have been found in clusters together with Cancer Associated Fibroblasts (CAFs). These clusters, which are also found containing other cell types as immune cells and platelets, are called Circulating Tumor Microemboli (CTMs). It is hypothesised that the CAFs play an important role in the metastatic process and the formation of the pre-metastatic niche. Therefore, it is important to study the formation and characteristics of these CAF-containing CTMs. However, these CTMs are extremely rare and difficult to extract and isolate. Therefore, studying patient samples is not viable. In-vivo models can be used to study specific characteristics of CTMs. However, to prepare CAF-containing CTMs, an accurate model of CAFs is also needed. In this study, several protocols described in literature to obtain CAF-like cells from Human Mammary Fibroblasts (HMFs) and the resulting CAFs will be compared.

1 Introduction

Cancer is a complex disease characterized by dysregulated cellular processes, especially cell division and cell death. Cancer cells arise from normal cells that undergo a series of genetic mutations or changes that disrupt the normal regulation of cell growth and division [1]. They acquire cancer specific characteristics, such as uncontrolled growth, immortality, sustained angiogenesis, genomic instability, escape from immune destruction and tissue invasion and metastasis [1] [2]. For some types of cancer, especially those diagnosed at an early stage

when the disease is localized and has not spread to distant organs, the prognosis can be quite favorable with appropriate treatment [3]. However, for cancers that have metastasized to distant sites, the prognosis is generally poorer, as metastatic cancer is often more difficult to treat and control. Metastatic cancer may require a combination of treatments, including surgery, chemotherapy, radiation therapy, targeted therapy or immunotherapy. [3].

Breast cancer has its own unique characteristics that can contribute to the potential for metastasis and the challenges associated with treating metastasis. Some of the most important characteristics of breast cancer are a high metastatic potential, heterogeneity of the cancer (widely different characteristics between cancer cells), difficulty in early detection and very supportive tumor Micro-environment (TME) [4].

Besides cancer cells, the TME consists of extracellular matrix (ECM), immune cells and Cancer Associated Fibroblasts (CAFs) among the various other components. CAFs are hypothesised to play a pivotal role in tumor progression, invasion, metastasis, and therapeutic resistance [5]. CAFs are a diverse population of stromal cells with altered phenotypes and functions compared to their normal counterparts. They contribute to tumor growth and progression through the secretion of growth factors, cytokines, ECM remodeling enzymes, and modulation of immune responses [6].

The transformation of normal mammary fibroblasts into CAF-like cells represents a critical event in breast cancer initiation and progression. Various factors in the TME, including transforming growth factor-beta 1 (TGF- β 1) and mechanical cues such as shear stress, have been implicated in driving the conversion of normal fibroblasts into CAFs [7]. In this study, we propose to leverage microfluidic technology to induce CAF-like characteristics in

HMFs through chemical and mechanical stimulation. Specifically, we aim to investigate the synergistic effects of TGF- β 1 and flow induced shear stress on the activation and differentiation of HMFs into CAF-like cells within a microfluidic chip. The resulting CAFs will in later studies be incorporated in clusters, containing circulating tumor cells (CTCs), immune cells and CAFs, to study the effect of CAFs on CTC survival in blood flow and metastatic potential.

2 Theoretical Background

2.1 The metastatic process

Cancer metastasis is a complex process involving a series of sequential steps that allow cancer cells to spread from the primary tumor site to distant organs throughout the body. Metastasis is the leading cause of mortality in breast cancer patients and represents a significant challenge in clinical management [3].

In figure 1 an overview of the metastatic process is visualized. The metastatic cascade can be broadly categorized into several key stages:

1. **Local Invasion:** Breast cancer cells acquire the ability to invade surrounding tissue through the degradation of the ECM. This process is facilitated by the secretion of proteolytic enzymes such as matrix metalloproteinases (MMPs) and the activation of signaling pathways that promote cell motility and invasion and lead to a more mesenchymal phenotype [8].

2. **Intravasation:** Once cancer cells breach the surrounding tissue, they enter nearby blood or lymphatic vessels through a process known as intravasation. This allows them to travel through the circulatory system to distant sites within the body. The mechanisms underlying intravasation involve interactions between cancer cells and endothelial cells lining the vessel walls, as well as changes in cell adhesion and cytoskeletal dynamics [8].

3. **Survival in Circulation:** Cancer cells face numerous challenges while circulating in the bloodstream or lymphatic system, including shear forces, immune surveillance, and anoikis (detachment-induced apoptosis) [5] [7]. To survive in circulation, cancer cells may undergo phenotypic changes, express pro-survival factors, and form clusters with other CTCs, endothelial cells, erythrocytes, stromal cells, platelets and immune cells, providing protection from immune attack and shear stress [5] [8].

4. **Extravasation:** Upon reaching distant organs, cancer cells must exit the bloodstream or lymphatic vessels to establish metastasis. This process, known as extravasation, involves interactions between cancer cells and the endothelium of capillary beds, as well as local microenvironmental cues that promote tumor cell

arrest and penetration into the surrounding tissue [7]. Breast cancer most commonly metastasize to bones, liver, lungs, and brain [2].

5. **Colonization and Growth:** Once extravasated, cancer cells adapt to the foreign microenvironment of the distant organ and initiate the formation of metastatic lesions. This often requires the activation of specific signaling pathways, such as those involved in cell proliferation, angiogenesis, and evasion of immune surveillance [8]. The establishment of metastatic colonies can lead to the development of secondary tumors that compromise organ function and contribute to disease progression [7].

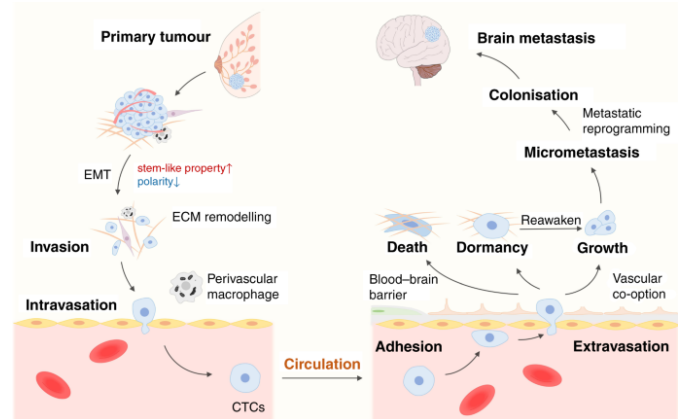


Figure 1: The metastatic process of breast cancer with a metastasis to the brain. [2]

2.2 CTM of CTCs with other cell types

CTMs represent a distinct population of circulating tumor entities comprised of 1-100 cancer cells, along with various stromal and immune cells. Unlike individual CTCs, which circulate singly in the bloodstream, CTMs exhibit a collective behavior, where multiple cell types are aggregated together.

Formation and Composition

CTMs can form through the aggregation of circulating cancer cells with CAFs, endothelial cells, erythrocytes, stromal cells, leukocytes, platelets and other blood components [9]. This process involves homotypic and heterotypic cell-cell interactions mediated by adhesion molecules, such as cadherins, integrins, and selectins, as well as secreted factors and extracellular vesicles [5]. The composition of CTMs can vary widely and may include cells of different phenotypes, genetic backgrounds, and metastatic potentials, as well as stromal and immune cells that contribute to the TME [5]. CAFs and platelets often are often found at the

surface of CTMs, providing protection from shear forces and immune surveillance [10].

Characteristics and Properties

CTMs exhibit increased resistance to anoikis and immune-mediated clearance compared to individual CTCs. Cell-cell contacts within clusters provide pro-survival signals and confer resistance to apoptotic stimuli [5].

CTMs have been associated with enhanced metastatic potential compared to single CTCs. The collective behavior of cells within clusters promotes their extravasation at distant sites and colonization of secondary organs, leading to more efficient establishment of metastatic lesions [5].

CTMs can evade immune surveillance by shielding cancer cells from immune recognition and attack. Platelets and the presence of CAFs at the surface of clusters can inhibit the activity of natural killer cells and promote immune evasion, while immune cells within clusters may exert immunosuppressive effects that facilitate immune escape [5].

CTMs exhibit functional interactions between different cell types within the cluster, including paracrine signaling, cell-cell communication, and metabolic cooperation [5]. These interactions may promote tumor growth, invasion, and metastasis by enhancing collective migration, ECM remodeling, and angiogenic signaling within the cluster [8].

Clinical Implications

The presence of CTMs in the bloodstream has been correlated with poor prognosis and increased risk of metastasis in cancer patients [7]. Detection and characterization of CTMs hold promise as prognostic biomarkers and may inform treatment decisions in the clinical management of cancer [5].

CTMs represent a potential therapeutic target for disrupting tumor metastasis and progression. Strategies aimed at targeting cluster formation, stability, or function may inhibit metastatic spread and improve clinical outcomes for cancer patients [7].

2.3 Role of CAFs in CTMs

CAFs are hypothesised to play a significant role within CTMs, contributing to their formation, stability, and functional properties.

Formation and Aggregation

CAFs promote the formation and aggregation of CTMs by interacting with cancer cells and other stromal cells within TME [5]. Through direct cell-cell contacts and secretion of ECM components, CAFs facilitate the adhesion and cohesion of cancer cells, promoting the formation of multicellular clusters [5] [9].

ECM Remodeling

CAFs are major contributors to ECM remodeling within TME. By secreting ECM-degrading enzymes such as matrix metalloproteinases (MMPs) and tissue inhibitors of metalloproteinases (TIMPs), CAFs promote the degradation of the basement membrane and ECM, facilitating cancer cell invasion and migration [10]. In the context of CTMs, CAF-mediated ECM remodeling can enhance cluster stability and facilitate collective migration of cancer cells within the bloodstream [5] [9].

Secretion of Pro-metastatic Factors

CAFs secrete various growth factors, cytokines, and chemokines that promote cancer cell survival, proliferation, and metastasis [6]. These factors include TGF- β , hepatocyte growth factor (HGF), fibroblast growth factor (FGF), and interleukins [9]. Within CTMs, CAF-derived factors can enhance the survival and metastatic potential of cancer cells, contributing to the aggressiveness of the cluster phenotype [10].

Immune Modulation

CAFs play a role in modulating immune responses within TME, which may also impact CTMs [9]. By secreting immunomodulatory factors such as interleukin-6 (IL-6), interleukin-8 (IL-8), and prostaglandin E2 (PGE2), CAFs can promote immunosuppression and inhibit anti-tumor immune responses [10]. This immunomodulatory function may contribute to immune evasion within CTMs, allowing them to evade immune surveillance and survive in the bloodstream [6].

2.4 Differences between CAFs and HMFs

CAFs and HMFs are both types of fibroblast cells found within the stromal compartment of cancerous

breast tissue, but they exhibit distinct differences in their characteristics and functions. HMFs are fibroblast cells native to normal breast tissue [6]. They maintain the structural integrity of the mammary gland and contribute to tissue homeostasis under normal physiological conditions. HMFs primarily contribute to the structural support and maintenance of normal mammary tissue structure. They participate in ECM synthesis and remodeling, provide mechanical support to epithelial cells, and regulate processes such as mammary gland development, lactation, and wound healing. [9].

CAFs are fibroblasts that have been activated and reprogrammed within cancerous tissues. They can originate from resident fibroblasts, mesenchymal stem cells, or other cell types such as endothelial cells or epithelial cells through a process known as fibroblast activation [9].

CAFs display a distinct gene expression profile compared to normal fibroblasts, characterized by upregulation of genes involved in ECM remodeling, cytokine secretion, and signaling pathways associated with cancer progression [9]. They often exhibit increased expression of markers such as α -smooth muscle actin (α -SMA) and fibroblast activation protein (FAP) [6]. CAFs play a critical role in promoting tumor growth, invasion, metastasis, and therapy resistance through various mechanisms [10]. They secrete growth factors, cytokines, and ECM-modifying enzymes that create a supportive micro-environment for cancer cells, stimulate angiogenesis, and suppress immune responses against tumors [9] [8].

Due to their pro-tumorigenic functions, CAFs are considered attractive targets for cancer therapy. Strategies aimed at targeting CAFs or modulating their activity have been explored as potential therapeutic approaches to disrupt the tumor-stromal interactions and inhibit cancer progression [10].

HMFs exhibit a thin, wavy, and small spindle morphology, CAFs appear as large, plump spindle-shaped cells with prominent nucleoli [11]. CAFs have more filopodia, Filopodia are thin and long membrane protrusions [12]. In figure 2 the difference in morphology between HMFs and CAFs is visualized.

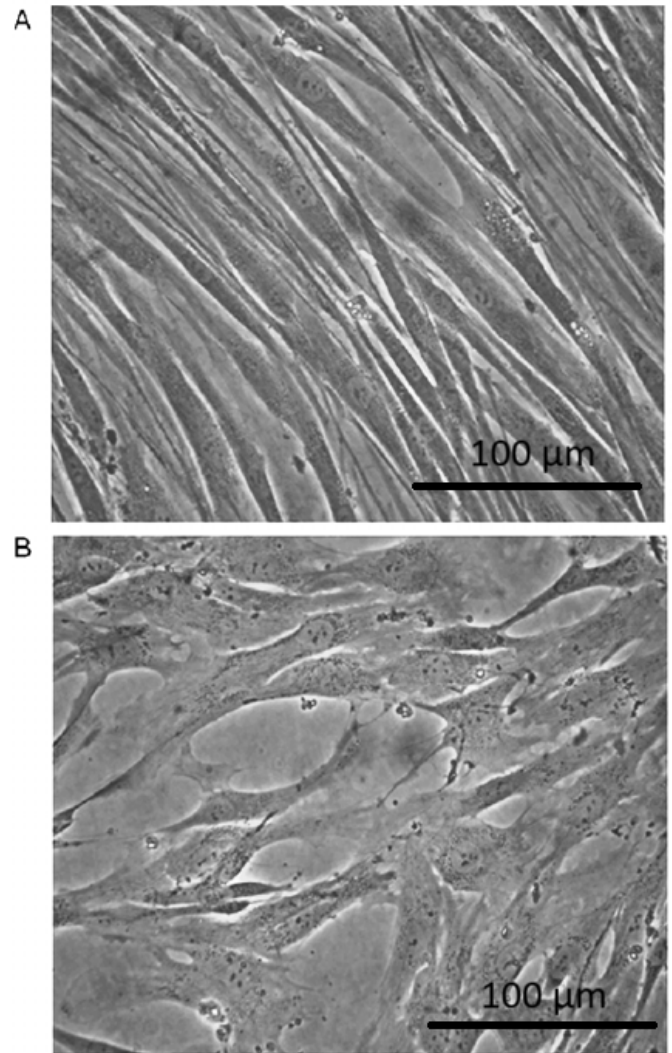


Figure 2: Morphology of isolated HMFs and tumor-derived fibroblasts. Light microscopic view showing the different morphology of fibroblasts isolated from human healthy mammary skin (A) or human breast cancer (B) samples after 6 days of culture. Picture from [13]

2.5 Inducing CAF-like characteristics in vitro

Because of the prominent role that fibroblasts have in wound healing, it is thought that key CAF-traits correspond to the normal physiological role of fibroblasts [9]. Several mechanisms can induce CAF activation. Contact between cancer cells and fibroblasts give rise to specific signals, such as TGF- β 1 production and Hippo pathways [2], that can lead to CAF activation. The stiffness and composition of the substrate and ECM can play a specific role in activation of fibroblasts; A higher stiffness will lead to more activation. DNA damage, physiological

stress, for example oxidation and mechanical stress, and the presence of inflammatory signals, such as IL-6, IL-9 and Tumor Necrosis Factor, can induce CAF-like characteristics in fibroblasts. The presence of TGF- β can also induce fibroblast activation [9].

The role of TGF- β 1 and physiological stress, in the form of fluid shear stress, will be further explained in the following sections. These two mechanisms will be used in the experiment for inducing fibroblast activation. Several studies have proven that the combination of fluid induced shear stress and TGF- β 1 can induce CAF-like characteristics and expression of key CAF-markers already after 6 - 24 hours of stimulation [14].

2.5.1 TGF- β 1

TGF- β 1 is a potent inducer of fibroblast activation, which is a key step in the differentiation of normal fibroblasts into CAFs [6]. In response to TGF- β 1 stimulation, fibroblasts undergo phenotypic changes characterized by increased proliferation, migration, and production of ECM components [9] [10].

One of the hallmark features of CAFs is the expression of α -SMA. This phenotypic transition is also critical for wound healing as well as CAF-mediated ECM remodeling and tumor-stromal interactions [9]. In wound healing the phenotypic change and the expression of α -SMA is regulated by TGF- β [15].

TGF- β 1 promotes the synthesis and deposition of ECM proteins such as fibronectin, collagen, and proteoglycans by CAFs [9]. This results in the remodeling of the ECM within the TME, that supports cancer cell invasion, migration, and metastasis [10].

TGF- β 1 stimulates CAFs to secrete various pro-tumorigenic factors, including growth factors (e.g., hepatocyte growth factor, fibroblast growth factor), cytokines (e.g., IL-6, IL-8), and MMPs [10]. These factors contribute to tumor progression by promoting cancer cell proliferation, angiogenesis, invasion, and immune evasion [6] [9].

CAFs also produce TGF- β 1, this can modulate immune responses within the TME [9]. It suppresses the activity of cytotoxic T cells and natural killer cells, promotes the differentiation of immunosuppressive regulatory T cells, and inhibits the function of antigen-presenting cells [15]. This immunosuppressive effect of TGF- β 1 contributes to immune evasion by cancer cells and facilitates tumor progression [10]. Crosstalk between CAFs and cancer cells within the TME can further enhance TGF- β 1 production by CAFs, leading to a feedforward loop that sustains

CAF activation and promotes tumor progression [15] [10].

Several studies found that stimulation with a concentration of 10 ng/mL TGF- β 1 for 6 - 24 hours was sufficient for inducing CAF transition in various types of fibroblasts [16] [14].

2.5.2 Shear Stress

Shear stress, and mechanical loading in general, can alter gene expression and lead to CAF-like characteristics in fibroblasts [17]. Fluid induced shear stress has emerged as a critical regulator of CAF differentiation and function within the TME [18].

Mechanical forces on cells leads to the activation of mechanotransduction pathways that sense and transduce mechanical cues into biochemical signals [17]. These pathways involve various mechanosensitive receptors, cytoskeletal components, and signaling molecules that modulate cellular responses to shear stress [19].

Shear stress in the form of flow has been shown to promote the activation and differentiation of normal fibroblasts into CAFs [20]. Studies have demonstrated that exposure of fibroblasts to shear stress leads to changes in cell morphology, cytoskeletal organization, and gene expression profiles characteristic of activated fibroblasts [19] [20].

A shear stress of above 0.1 dyne/cm² on fibroblast cells already can induce activation of Mechanotransduction Pathways [17]. A shear stress between 2 - 10 dyne/cm² for 6 - 24 hours will effect in a differentiation to CAFs [19] [14] [16]. Interstitial fluid shear stress may be as low as 0.1 dyne/cm², but CTMs exposed to vascular blood flow can experience fluid shear stress up to 30 dyne/cm² [18].

Remodelling of the ECM by CAFs is stimulated by shear stress [17]. CAFs subjected to shear stress exhibit increased synthesis and deposition of ECM proteins, such as collagen, fibronectin, and proteoglycans, leading to ECM remodeling and fibrotic changes that support tumor progression [19].

Shear stress activates signaling pathways in CAFs that promote their pro-tumorigenic functions [17]. For example, shear stress-induced activation of focal adhesion kinase (FAK), mitogen-activated protein kinase (MAPK), and nuclear factor kappa B (NF- κ B) pathways in CAFs can enhance the secretion of growth factors, cytokines, and MMPs that support tumor growth, invasion, and metastasis [19].

Angiogenic processes within the TME are regulated by shear stress, by modulating the secretion of angiogenic factors by CAFs. Shear stress-induced expression of angiogenic factors such as vascular endothelial growth

factor (VEGF) and angiopoietin-1 (Ang-1) promotes endothelial cell proliferation, migration, and tube formation, leading to enhanced tumor vascularization and angiogenesis [17].

2.5.3 Microfluidics and shear stress

Microfluidic chips offer a powerful platform for applying controlled shear forces on cells in culture.

However, in the context of microfluidics (channels of micrometer dimensions) and especially in rectangular channels, the flow velocity profile and the resulting shear stress are complex. The wall shear stress is not uniform and undergoes variations along the top, bottom, and side walls of the channel. However, the geometry can be simplified by imagining two infinite parallel plates instead of enclosed channels. Under this simplified assumption, the average shear stress can be described by the following equation [19]: $\tau = \frac{6\eta Q}{h^2 w}$. Which leads to the equation for the flow: $Q = \frac{\tau h^2 w}{6\eta}$. Where Q is the flow rate [$\frac{mL}{s}$], τ is the shear stress [$\frac{dyne}{cm^2}$], h the channel height [cm], w the channel width [cm] and η the dynamic viscosity [$dyne*s/cm^2$]. The dynamic viscosity is dependent on the temperature, pressure and the composition of the fluid. Cell culture medium with 10% Fetal Bovine Serum (FBS) at 37° Celsius has a dynamic viscosity of 0.00958 $dyne*s/cm^2$ [21].

3 Materials and Methods

3.1 Microfluidic chip

In SolidWorks (Dassault Systèmes SolidWorks Corp, Waltham, MA, USA) a mould for the chips was designed. With a stereo lithography (SLA) 3D printer the mould was printed, using the Form3+ (Formlabs, Somerville, MA, USA) SLA 3D Printer and the clear resin V4 (Formlabs). The chips were made by casting Polydimethylsiloxane (PDMS) in the mould and then plasma bonded to a glass slide using the CUTE Plasma System plasma cleaner (Femto Science Inc., Gyeonggi, Korea).

3.1.1 Chip designs

Two different chip were designed. The second version has been used in the experiments due to impracticality's of the first version, such as difficulty with harvesting the cells out of the chip and difficulty with fixating and staining the cells.

In Figure 3, the first version of the chip can be seen. The diameter of the in- and outlets are 4 mm. The

height of the channel is 500 μm . The surface area of the channel is 3.9 cm^2 , the in- and outlet excluded. The volume of the chip is 195 μL . The mould was designed to make 4 chips at a time.

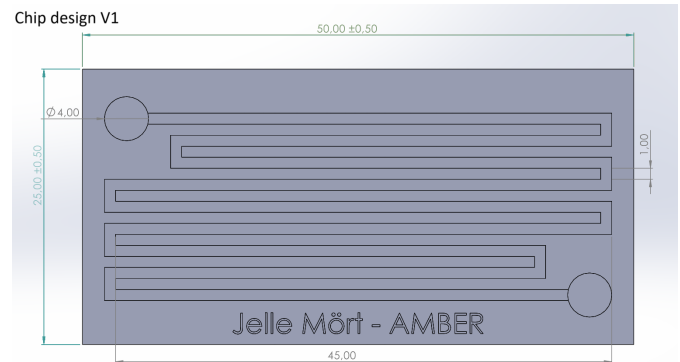


Figure 3: Design of the first chip, made in SolidWorks. Units are in mm.

In Figure 4, the second version of the chip can be seen. The chip was designed to have one condition per chip, so it tests the condition in triplicates. The diameter of the in- and outlets are 4 mm. The height of the channel is 500 μm . The surface area of the channel is 1.68 cm^2 , the in- and outlet excluded. The volume of one channel is 84 μL . The mould was designed to make 4 chips at a time.

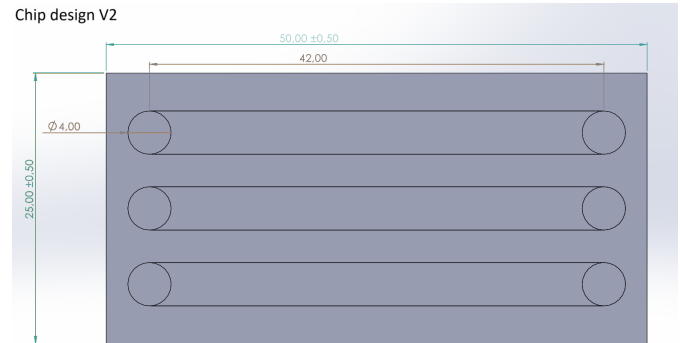


Figure 4: Design of the second chip, made in SolidWorks. Units are in mm.

The second chip design was chosen for the experiments. This design had more advantages, such as one chip for one condition in triplicates, easier harvesting of cells and easier staining and imaging of the cells.

3.1.2 SLA printing of chip mould

Using the Form3+ SLA 3D printer the mould was printed with clear resin V4. After printing, the mould was washed in the ultrasonic cleaner (Formlabs) with isopropanol for 30 min (15 min each side). After cleaning, the mould was cured with UV for 60 min at 60° Celsius in the Cure machine (Formlabs).

Mixing PDMS

The required amounts of PDMS base and curing agent were measured to the ratio of 10:1 by weight. The PDMS base and curing agent were thoroughly mixed in a plastic mixing cup. The mixture was stirred until it was homogeneous.

Degassing

Degassing the PDMS mixture removes any trapped air bubbles that could cause imperfections in the final cast. To degas the mixture, it was placed in a vacuum desiccator for 1 hour at -0.08 bar. This process will cause any air bubbles to rise to the surface and escape. Once the mixture was bubble-free, it was stored in a freezer or used immediately.

Casting PDMS

When the PDMS mixture was ready for use, it was poured into the prepared mould. The PDMS was slowly and steadily poured into the mould to avoid trapping any air bubbles. Once the mold was filled, it was placed in a vacuum desiccator for 1 hour at -0.08 bar. Then to cure the PDMS, the mould was placed in an oven set to 65 °C overnight.

Demolding

Once the PDMS was cured, it was removed from the mould. The PDMS slab was cut into the 4 chips and excess PDMS was cut away. The in- and outlets were punched using a PDMS puncher with a diameter of 4 mm. To prevent dust formation on the chips, tape was used to cover the top and bottom of the PDMS chips.

3.1.3 Plasmabonding

Plasma Treatment

Plasma bonding involves subjecting the surfaces to a low-pressure, glow discharge plasma environment. The plasma activates the surfaces by introducing reactive oxygen groups, enhancing their affinity for bonding. The plasma treatment utilizes oxygen to form the

plasma.

The glass slide and PDMS chips were placed in the plasma cleaner, with the side that will be bonded facing upwards. A duration of 45 seconds and a power of 50 W was used. After plasma activation, the oxidized PDMS was positioned on top of the glass slide. To prevent potential weakening of the bond over time, this procedure was executed fast. Then, the chip was incubated for a minimum of one hour at 65°C to enhance the bonding strength.

3.2 Cell culture

Primary cultured human mammary fibroblast cells were purchased from ScienCell (ScienCell Research Laboratories, CA, USA) and maintained in complete Fibroblast Medium (FM) (ScienCell) containing 10% Fetal Bovine Serum (FBS) and 1% Penicillin-Streptomycin and fibroblast growth supplement (FGS). Cells were grown in a Poly-L-Lysine (coating density of 2 $\mu\text{g}/\text{cm}^2$) coated T-75 culture flask, to minimize fibroblast activation, and incubated in a 37°C, 5% CO₂ incubator.

3.2.1 Maintaining cell line

When the cells reached 95% confluency in the T-75 culture flasks the cells were passaged into the next coated flask. 0.05% Trypsin/Ethylenediaminetetraacetic acid tetrasodium salt dihydrate solution (T/E solution) was used to detach the cells from the flask. Once the cells were harvested and placed in a 50 ml tube, filled with 5 mL FBS beforehand, and 10 mL trypsin neutralising solution (TNS) (ScienCell) + Cell suspension, the cell suspension was centrifuged at 1000 RPM for 5 minutes. The cell pellet was re-suspended with 5 mL of FM. The cell concentration was determined with the EVE automated cell counter (NanoEntek). The cells were seeded in a poly-L-lysine (coating density of 2 $\mu\text{g}/\text{cm}^2$) coated T-75 flask with a seeding density of 5,000 cells/cm². The rest of the cell suspension was used for seeding the cells in the chips.

3.2.2 Seeding cells in chips

The chips were cleaned with an UV (405 nm) treatment of 30 min. The chips were coated with 2 $\mu\text{g}/\text{cm}^2$ poly-l-lysine coating in each channel for 15 min. Then the chips were coated with fibronectin with a concentration of 20 $\mu\text{g}/\text{mL}$ for 1 hour. The cells were seeded with a seeding density of 3 x 10⁴ cells/cm², to ensure a mono-layer of cells [19]. The in- and outlets were filled with fibroblast medium, to ensure that the

channels do not dry out. The chips were incubated overnight in a 37 °C, 5% CO₂ incubator.

3.3 Experiment

3.3.1 Preparing chips for experiment

The chips were prepared for experimentation, using MasterFlex L/S 14-tubing (Masterflex SE, Gelsenkirchen Germany).

Initially, the chips were inspected under a microscope to verify cell adhesion.

Then, in a laminar-flow cabinet, the channel-to-channel tubing was connected. The outlet of channel 1 was connected to the inlet of channel 2, in figure 5 the in-outlets that are marked 1. The same was done with the outlet of channel 2 and the inlet of channel 3, in figure 5 the in-outlets that are marked 2. In figure 6 the final result is seen. The channels were linked in series for optimal fluid flow and an identical flow rate in all the channels.

A medium containing TGF- β 1 was prepared by adding TGF- β 1 to complete fibroblast medium to a final concentration of 10 ng/mL. A reservoir for circulation was filled with this solution and incubated for 15 min to avoid bubble formation.

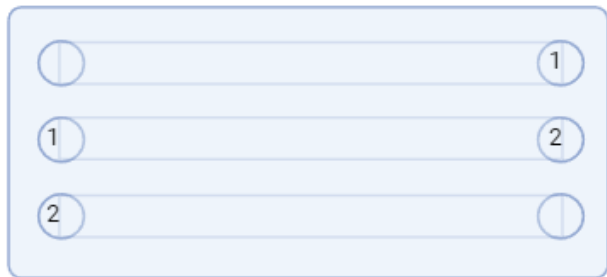


Figure 5: Picture of the positions of the Masterflex L/S 14 Tubing to have the channels in series in the second version of the chip.

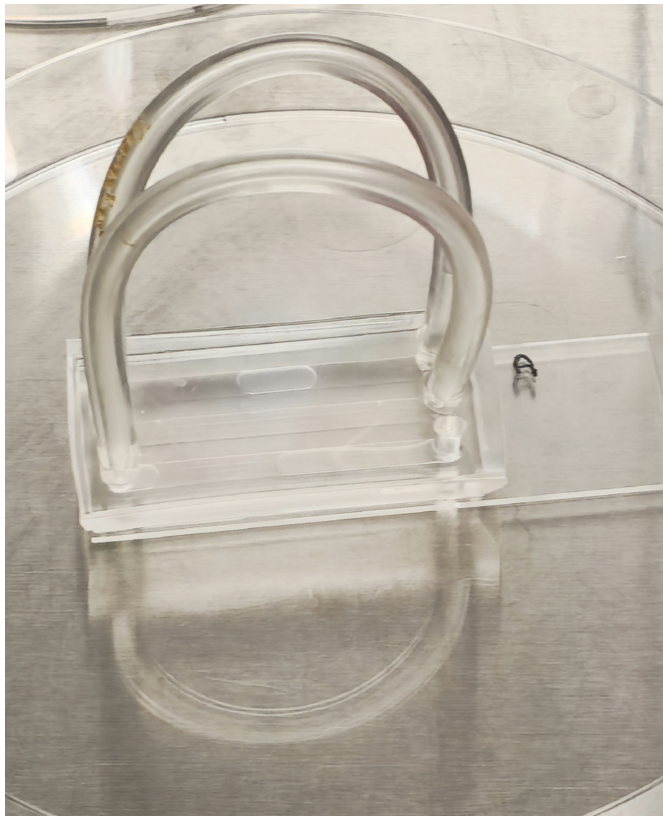


Figure 6: Picture of the positions of the Masterflex L/S 14 Tubing to have the channels in series in the second version of the chip.

3.3.2 Starting experiment

In the experiment, a peristaltic pump from MasterFlex/Cole Parmer (Masterflex SE) was utilized in combination with the MasterFlex L/S 14-tubing (Masterflex SE).

Initially, the Reservoir-to-pump tubing was connected and filled with the FM + TGF- β 1 mixture by starting the pump. The pump was stopped when the medium almost filled the tubing.

Then, the tubing was connected to the inlet of channel 1 of the chip. Simultaneously, the outlet-to-reservoir tubing was connected to the outlet of channel 3, with the end of the tubing placed in the reservoir to establish a continuous flow pathway. In figure 7 a visualization of the setup is depicted.

The pump was then started at a flow rate of 0.3 mL/min, and any air bubbles were removed by gently pressing on the tubing. Once all bubbles were eliminated, the experiment was initiated at 10.8 mL/min flow rate to have a fluid induced shear stress of around 10 dyne/cm².

After 15 hours the experiment was stopped by turning off the pump.

The Reservoir-to-pump and the outlet-to-reservoir tubing were cut 3 mm above the chip, leaving the channel-to-channel tubing intact. Similarly, the channel-to-channel tubing was cut in a laminar-flow cabinet, also 3 mm above the chip.

Under the microscope, the channels were inspected for the presence of cells.

Depending on the subsequent steps, preparations were made either for cell lysis for qPCR analysis or for fixation for (immuno)staining.

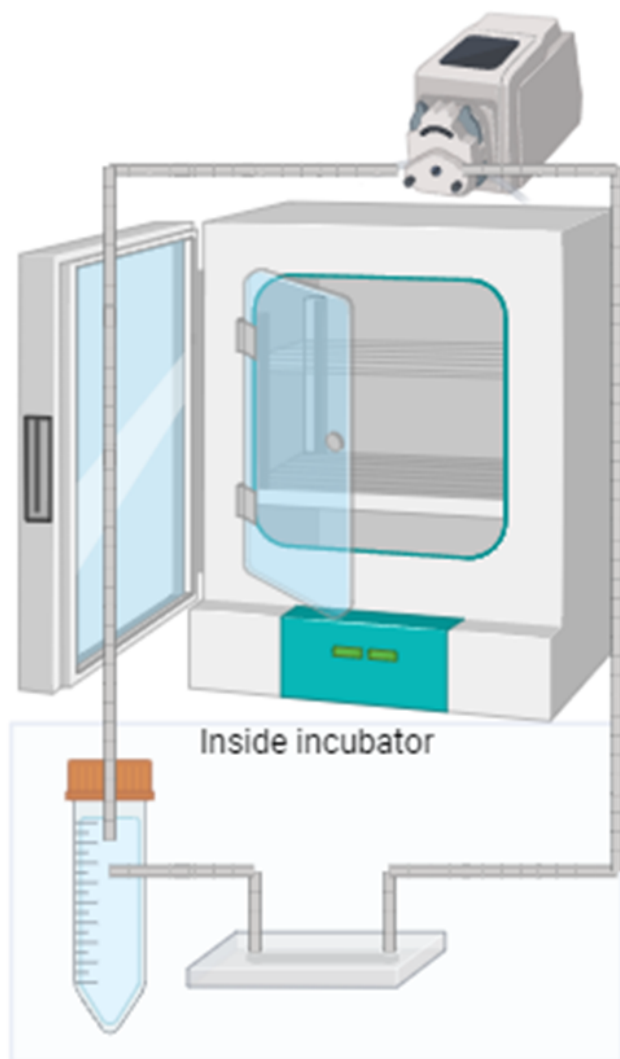


Figure 7: Visualization of the setup of the experiment. A peristaltic pump on top of an incubator with tubing connecting the reservoir and chip for a continuous flow pathway. Made in BioRender.

3.4 Analysis

Staining

To visualize the change in expression of

certain proteins or the change in morphology, (immuno)staining can be used. To visualize the nuclei of the cells, 4,6-diamidino-2-phenylindole (DAPI) (Excitation/Emission: 358/461 nm) (1mg/ml stock concentration) (ThermoFisher scientific) was used to stain the nuclei. To look at the morphology and cell shape, Texas Red-X Phalloidin (Excitation/Emission: 591/608 nm) (2,000 assays/mL stock solution) (ThermoFisher scientific) was used to stain F-actin. Immunostaining with mouse anti- α -SMA (0.5 mg/mL stock concentration)(Bio-Techne) primary antibodies and rabbit anti-mouse Alexa Fluor 488 (Invitrogen) secondary antibodies were used for α -SMA staining.

Cells in the chip were fixed with 4% formaldehyde(Formol) for 15 minutes at room temperature. Followed by 3 washing steps with PBS. Then, cells were permeabilized with 0.1% Triton-X 100 solution for 20 minutes. After permeabilization the cells were blocked with 1% BSA solution, to prevent unspecific binding, for 1 hour at room temperature. After blocking the samples were incubated at 4 °C overnight with primary antibodies using mouse anti- α -SMA (Bio-Techne) at 1:100 dilution. After incubation, samples had 3 washing steps with PBS and were labeled with secondary antibodies using rabbit anti-mouse Alexa Fluor 488 (Invitrogen) 1:200 dilution for 1 hour at room temperature. Cell nuclei and F-actin were stained with DAPI (Invitrogen) and Texas Red-X Phalloidin (Invitrogen) respectively. This was done at 1:200 dilution for 15 minutes at room temperature.

Morphology & Directionality

To investigate if the cells were affected by the flow, a directionality analysis was performed using ImageJ. From the intensity and direction of the F-actin fibers a vector field can be made with the help of the directionality function in ImageJ. From this vector field a graph can be made that shows the angle with respect to the flow direction. If the cells are aligned with the flow then the flow had an effect on the cells.

The morphology change of the cells was examined with a light microscope and an EVOS fluorescence microscope (Invitrogen, Thermo Fisher Scientific Corporation, MA, USA). The morphology change was highlighted using DAPI and Phalloidin staining, to stain the nuclei and F-actin respectively.

qPCR

For the RNA extraction the RNeasy micro kit (Qiagen) was used. This kit can be used for qPCR when there are less than 500,000 cells present. With the chemical and mechanical stimulation in mind, the genes in table 1 will be looked at with quantitative Polymerase Chain

Reaction (qPCR) analysis. For the housekeeping genes GAPDH, B2M and RPL13A were used.

The delta-delta Ct method was used to calculate the fold gene expression, to validate the significance of the data a T-test was done to provide a P-value [22].

4 Results

In figure 8 the bright-field microscope pictures are seen. A is the control without flow and TGF- β 1. B is the control with TGF- β 1 and without flow. C is the experiment with a flow of 10.8 mL/min (shear stress of 10 dyne/cm²) for 15 hours with TGF- β 1. There is a different morphology between the control groups (A and B) due to the presence of TGF- β 1. A CAF-like morphology can be seen in C, the cells are spread out, have more filopodia and are large spindle shaped. The cells grew in the direction of the flow.

In figure 9 typical CAF morphology is seen after stimulation with flow induced shear stress (10.8 mL/min; 10 dyne/cm²) and TGF- β 1 for 15 hours, for example more filopodia are present in these cells, large spindle shape and the cell is spread out.

In figure 10 the difference of directionality of the cells between the control group (A) and the experiment (B) are significant. There is a clear difference in the cell alignment. In B the cells under flow will align with the flow direction.

In figure 11 the pictures taken with the EVOS are shown. In blue the nuclei are stained with DAPI. In red the F-actin is stained with Texas Red. In green the α -SMA is stained with AlexaFluor-488. A is the control without flow and without TGF- β 1. B is the control with TGF- β 1 and without flow. C is the experiment with TGF- β 1 and with a flow of 10.8 mL/min (shear stress of 10 dyne/cm²) for 15 hours. An increased intensity of α -SMA is seen in the experiment (C) with respect to the control groups (A and B). To better see this only the α -SMA expression is shown in figure 11 as D,E and F. The intensity of F-actin is also higher in the experiment (C) with respect to the control groups (A and B).

In figure 12 the fold gene expression graphs are shown for α -SMA, FAP, MMP-2 and COL1A1 expression. For α -SMA an increased expression is seen when TGF- β 1 is added. An even stronger increase is present when a flow is added. An increase of FAP expression is seen in the cells of the experiment with respect to the control groups. There is a slight decrease in expression when only TGF- β 1 is added. There is an increase of COL1A1 expression in the experiment with respect to the control groups. A slight decrease is seen when only TGF- β 1 is added. For α -SMA there is a

slight decrease in expression when TGF- β 1 is added. When a flow is added, there is a further decrease in expression.

The results of the T-test, to see if the results are of significance, are in table 2. For all the genes the P-values are lower than 0.05, which means that the difference in gene expression is of statistical significance.

Table 2: P-value obtained by using T-test on the Cq values from the qPCR. P-values lower than 0.05 show statistical significance.

Genes	P-value
Alpha-SMA	0,0006
FAP	0,03
MMP-2	0,0063
COL1A1	0,005

5 Discussion

In this study in vitro differentiation of HMFs to induce CAF-like characteristics was tested, with TGF- β 1 and fluid shear stress as stimulation. The resulting CAF-like cells are intended for further in vitro studies on the roles of CAFs in metastasis.

Development of a method to put controlled shear flow on HMF cells for prolonged time was made. The induction of CAF-like characteristics were tested using (immuno)staining and qPCR. To validate the effect of flow on the cells directionality test was done.

The morphology of the HMFs after stimulation were compared to the morphology of CAFs in literature. When the cells with flow in figure 8 (C) are compared to the CAFs in figure 2 (B), there are many similarities. The cells have a large spindle shape, are more spread out and have more filopodia compared to the normal fibroblasts. This change in morphology is also present in the cells in figure 9. // // Analysis of (immuno)staining showed a significantly higher presence of α -SMA in the cells with flow shear on them, with respect to the control groups. Some control groups, without flow and without TGF- β 1, also showed a slight presence of α -SMA, this is probably due to other kind of stimulation. Such as a lower cellular health in higher passage numbers, cell culture on plastic, the coating used in the experiments or activation via cell-produced TGF- β 1, that is produced via the wound healing pathway. This was also seen in other studies [23].

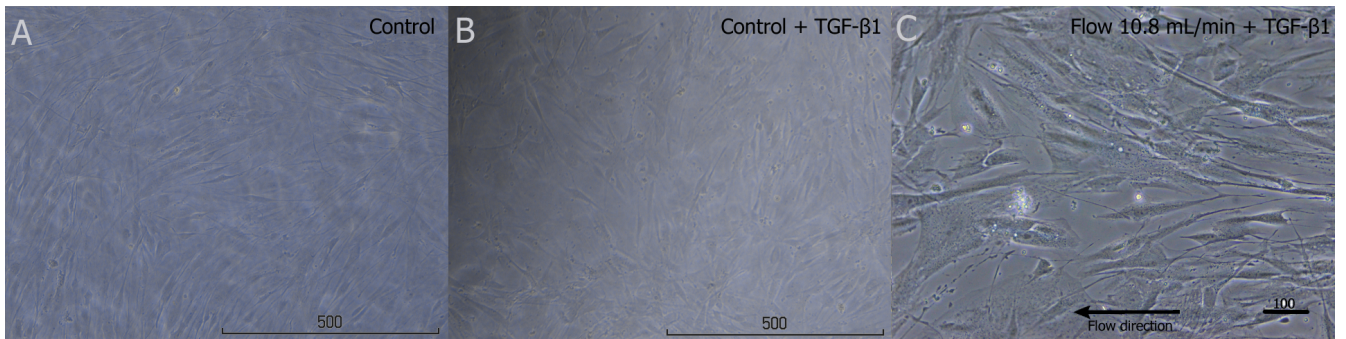


Figure 8: Pictures of the cells with a bright field microscope. A: Control without flow and TGF- β 1. B: Control without flow + TGF- β 1. C: Experiment with 15 hours of flow (10.8 mL/min; Shear Stress of 10 dyn/cm²). Scale-bar is in micrometers.

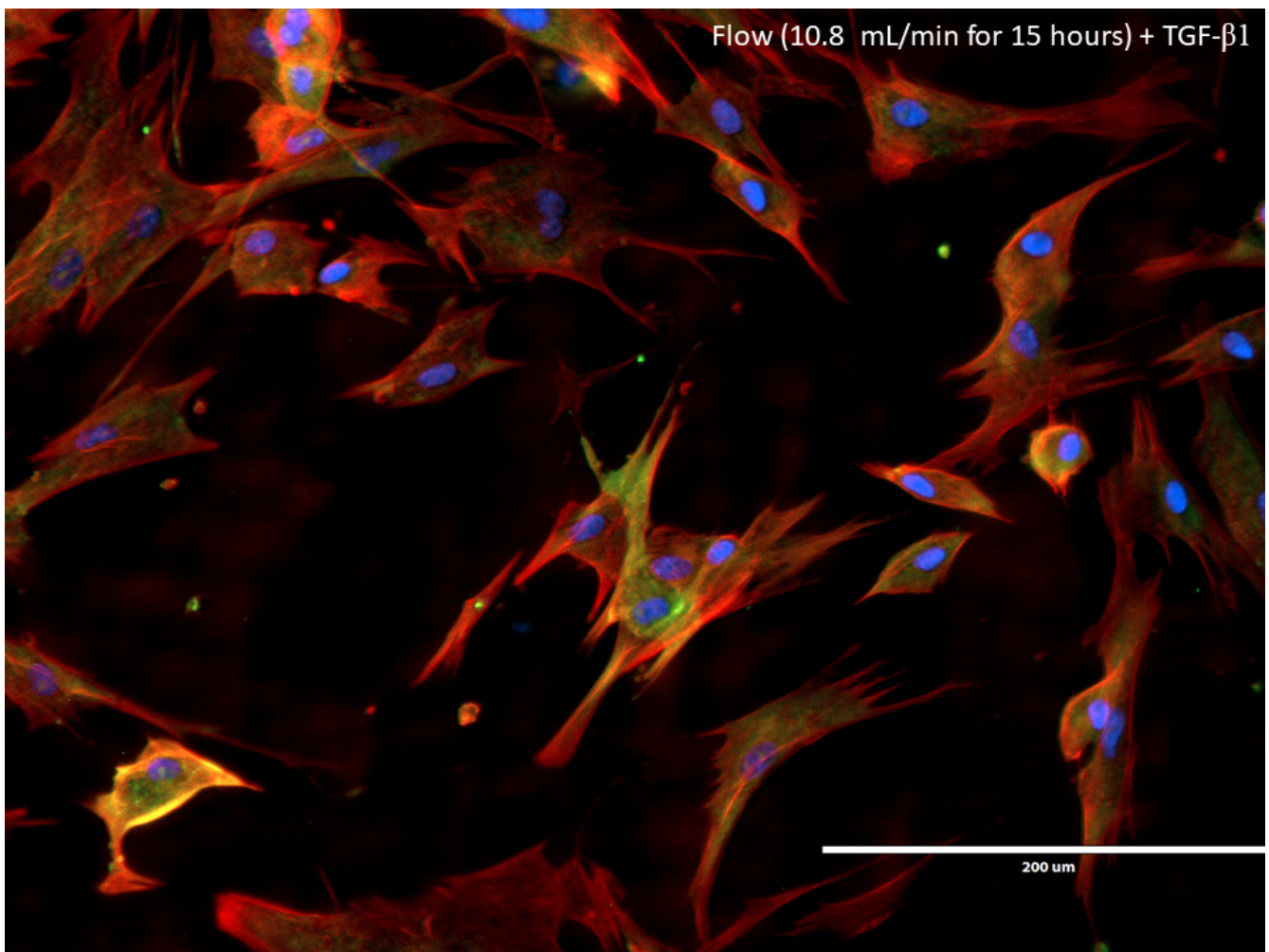


Figure 9: A EVOS picture of the cells with flow and with TGF- β 1 for 15 hours. The pictures are made with with the same settings with the EVOS microscope, so direct comparison is possible. In blue the nuclei are stained with DAPI. In red the F-actin is stained with Phalloidin Texas Red. In green is the α -SMA stained with AlexaFluor-488.

Table 1: Genes of interest and housekeeping genes used for qPCR analysis.

Genes	Expression	Forward Sequence	Reverse Sequence
a-SMA	+	TGGACGCACAACCTGGCAT	AATAGCCACGCTCAGTCAGG
FAP	+	AGTCCAGAATGTTTCGGTCCG	TTCTATATGCTCCTGGGTCTTTGG
MMP-2	+	TACGATGGAGGCGCTAATGG	TGTGTAGCCAATGATCCTGTATGT
COL1A1	+	GTCACCCACCGACCAAGAAACC	AAGTCCAGGCTGTCCAGGGATG
Housekeeping genes			
GAPDH		CGCTCTCTGCTCCTCCTGT	CCATGGTGTCTGAGCGATGT
B2M		GACTTGTCTTTCAGCAAGGA	ACAAAGTCACATGGTTCACA
RPL13A		AAAAAGCGGATGGTGGTTC	TACTTCCAGCCAACCTCGT

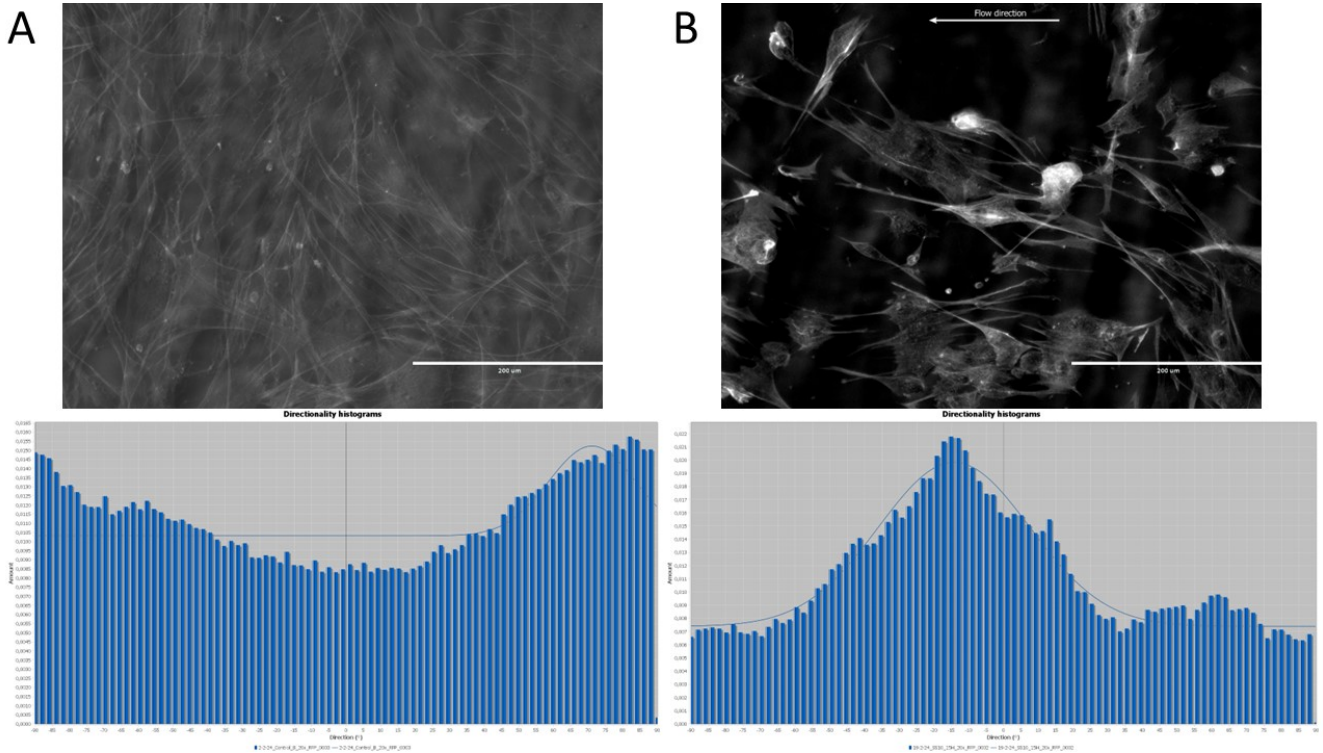


Figure 10: Directionality analysis of the control group (A) and the experiment (B) using the directionality function in ImageJ. On the X-axis the angle with respect to the flow direction and on the Y-axis the amount of F-actin fibers in a certain direction.

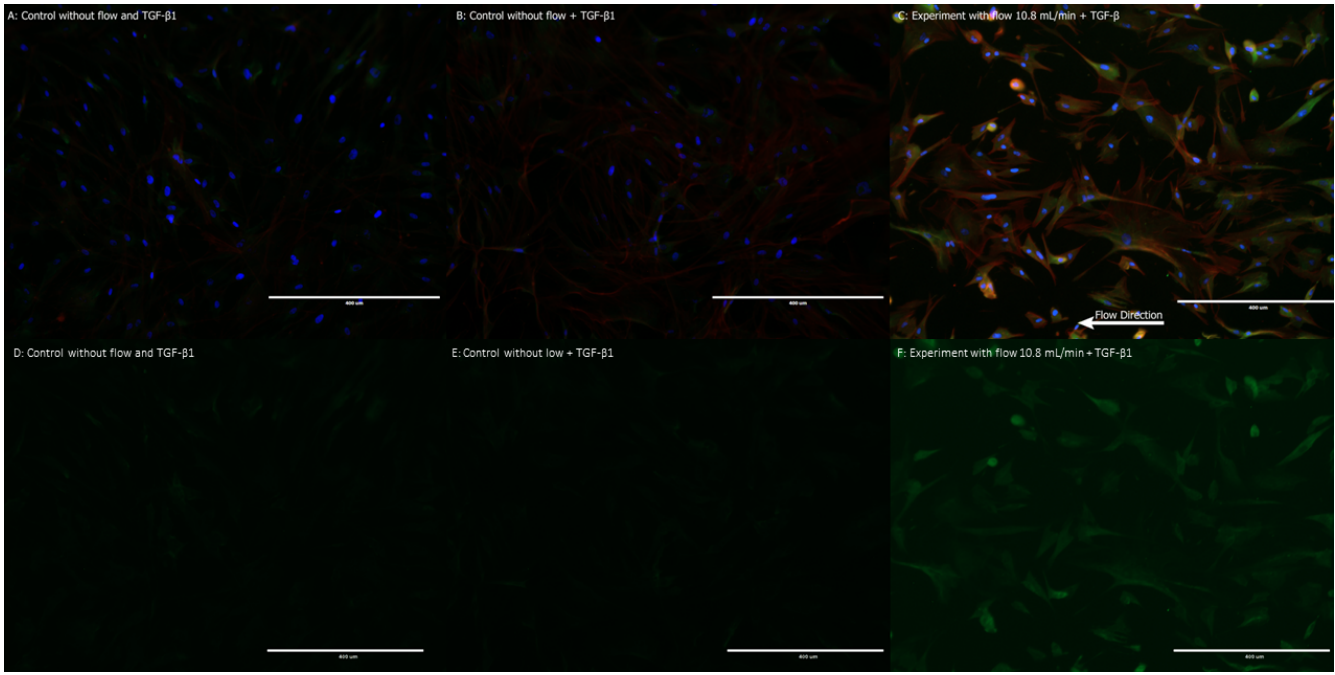


Figure 11: A: the control group without flow and without TGF-Beta1. B: the control group without flow and with TGF-β1. C: the experiment with flow and with TGF-β1. D,E and F are the same pictures but only the α-SMA is depicted. All pictures are made with with the same settings with the EVOS microscope, so direct comparison is possible. In blue the nuclei are stained with DAPI. In red the F-actin is stained with Phalloidin Texas Red. In green the α-SMA is stained with AlexaFluor-488.

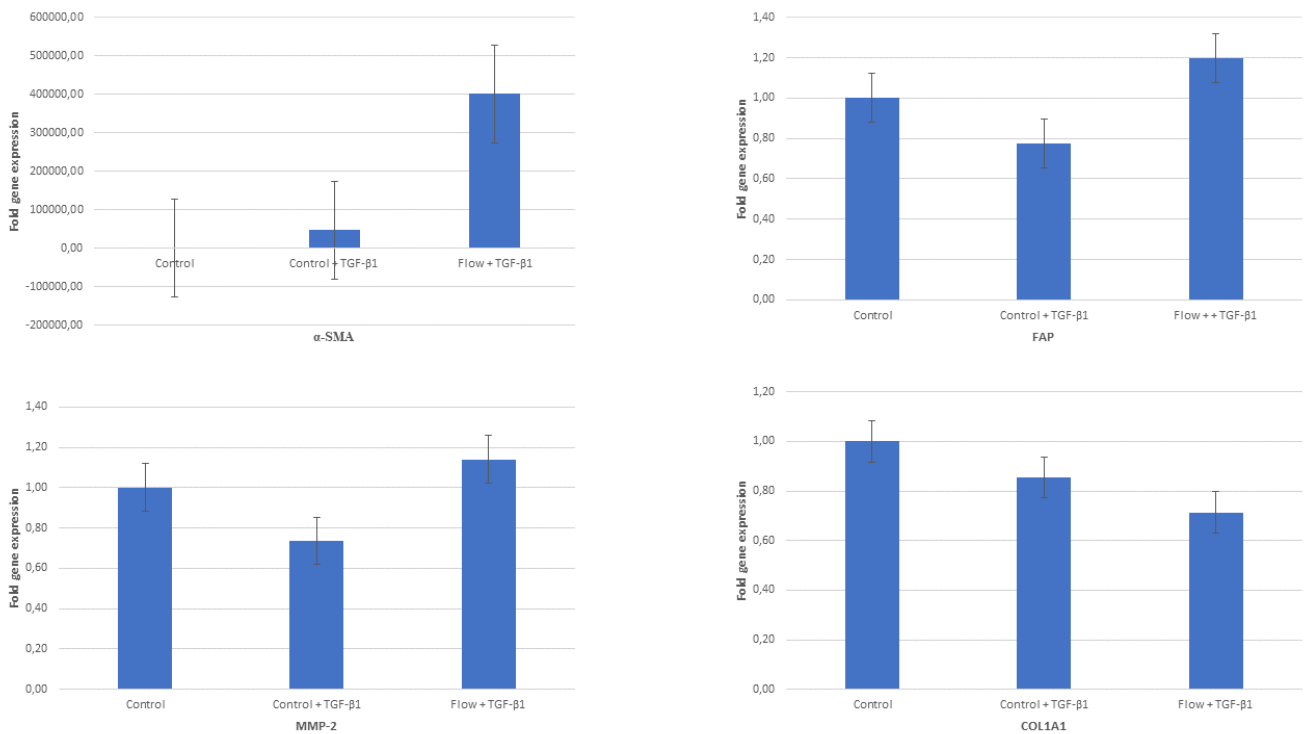


Figure 12: Results of the qPCR. The fold gene expression was calculated with the delta-delta Cq method. α-SMA, FAP, MMP-2 and COL1A1 expression was tested using qPCR analysis, RPL13A was used as a housekeeping gene.

Analysis by qPCR showed an increase of expression in α -SMA, FAP and MMP-2 and a decrease in COL1A1 expression in the cells with flow. The decrease of FAP, MMP-2 and COL1A1 in the control group with TGF- β 1 is due to the myofibroblast activation, the same effect of only TGF- β 1 is seen in wound healing [24]. So the increase of α -SMA, FAP and MMP-2 expression in the flow group, indicates a more CAF-like expression when flow and TGF- β 1 are present. The lower COL1A1 expression can be explained by the fact that different CAF sub-types have different expression of certain genes [9]. To check for Collagen expression, a different type of collagen can be examined in qPCR analysis.

There was significantly more cDNA than expected and measured with the Nanodrop. Therefore the amount of cycles needed to overcome the threshold during qPCR was very low. So the expression of FAP, MMP-2 and COL1A1 looked, at first, very similar, but this is likely due to the very low cycles needed to overcome the threshold.

In this study only 15 hours of flow and TGF- β 1 treatment was done. Differentiation is a slow process. In literature the time of treatment varies between 6 and 48 hours [16] [18]. In future experiments longer and shorter differentiation times should be applied.

Only a selection of markers was studied. CAFs are highly heterogeneous with many descriptions appearing in literature. A more comprehensive study of CAF markers will provide a better indication of CAF markers induced by fluid shear stress.

In this study we used only HMFs. Different cells of origin for CAFs, for example other fibroblasts, endothelial cells and macrophages can also differentiate towards CAFs, can also be included to study the effect of fluid shear stress on CAF differentiation of cells of different origins.

This was only the first step of a future study including CAFs in CTMs to study the roles of different cell types in CTMs during the metastatic process.

This was only a pilot study to analyse the effects of flow induced shear stress on HMFs. In further studies control samples without TGF- β 1 but with flow should be included, to better evaluate the effect of flow induced shear stress on HMFs. Also the shear stress should be varied, by changing the flow rate, to study the various flow conditions.

6 Conclusion

In this study the influence of shear stress on HMFs to induce CAF-like characteristics was researched. We have seen that there is an increase of expression of the key markers for CAFs in the cells with flow induced shear stress and TGF- β 1 stimulation with respect to the control groups. So, the method that was made is a promising first step for further studies to include these CAF-like cells in CTMs to model the survival and metastatic potential of CTMs in blood-flow and the role of the different cell types in CTMs.

Acknowledgements

I would like to thank every member of AMBER; especially dr. ir. Kirsten Pondman and prof. dr. ir. Séverine Le Gac for the opportunity to be able to do my bachelors assignment at AMBER. I want to thank prof. dr. Robert Passier for being the external member of the committee. Special thanks to Franck Assayag for all the support during my assignment.

References

- [1] Hanahan D, Weinberg RA. The hallmarks of cancer. *Cell*. 2000 Jan;100(1):57–70.
- [2] Wang Y, Ye F, Liang Y, Yang Q. Breast cancer brain metastasis: insight into molecular mechanisms and therapeutic strategies. *British Journal of Cancer*. 2021 Oct;125(8):1056–1067.
- [3] Dillekås H, Rogers MS, Straume O. Are 90% of deaths from cancer caused by metastases? *Cancer Med*. 2019 Aug;8(12):5574–5576.
- [4] Li CI, Uribe DJ, Daling JR. Clinical characteristics of different histologic types of breast cancer. *British Journal of Cancer*. 2005 Oct;93(9):1046–1052.
- [5] Lin SLLMea D. Circulating tumor cells: biology and clinical significance. *Sig Transduct Target Ther* 6, 404. 2021 Oct. doi:<https://doi.org/10.1038/s41392-021-00817-8>.
- [6] Xing F, Saidou J, Watabe K. Cancer associated fibroblasts (CAFs) in tumor microenvironment. *Front Biosci (Landmark Ed)*. 2010 Jan;15(1):166–179.
- [7] Ildiz ES, Gvozdenovic A, Kovacs WJ, Aceto N. Travelling under pressure - hypoxia and shear stress in the metastatic journey. *Clinical & Experimental Metastasis*. 2023 Oct;40(5):375–394.

- [8] Drapela S, Gomes AP. Metabolic requirements of the metastatic cascade. *Curr Opin Syst Biol.* 2021 Sep;28.
- [9] Sahai E, Astsaturov I, Cukierman E, DeNardo DG, Egeblad M, Evans RM, et al. A framework for advancing our understanding of cancer-associated fibroblasts. *Nature Reviews Cancer.* 2020 Mar;20(3):174–186.
- [10] Glabman RA, Choyke PL, Sato N. Cancer-Associated Fibroblasts: Tumorigenicity and Targeting for Cancer Therapy. *Cancers (Basel).* 2022 Aug;14(16).
- [11] Gascard P, Tlsty TD. Carcinoma-associated fibroblasts: orchestrating the composition of malignancy. *Genes Dev.* 2016 May;30(9):1002–1019.
- [12] Franchi M, Piperigkou Z, Riti E, Masola V, Onisto M, Karamanos NK. Long filopodia and tunneling nanotubes define new phenotypes of breast cancer cells in 3D cultures. *Matrix Biology Plus.* 2020;6-7:100026. Complexity of Matrix Phenotypes. Available from: <https://www.sciencedirect.com/science/article/pii/S2590028520300077>. doi:<https://doi.org/10.1016/j.mbplus.2020.100026>.
- [13] Angelucci C, Maulucci G, Lama G, Proietti G, Colabianchi A, Papi M, et al. Epithelial-Stromal Interactions in Human Breast Cancer: Effects on Adhesion, Plasma Membrane Fluidity and Migration Speed and Directness. *PLOS ONE.* 2012 12;7(12):1–13. Available from: <https://doi.org/10.1371/journal.pone.0050804>. doi:10.1371/journal.pone.0050804.
- [14] Molladavoodi S, Robichaud M, Wulff D, Gorbet M. Corneal epithelial cells exposed to shear stress show altered cytoskeleton and migratory behaviour. *PLOS ONE.* 2017 06;12(6):1–16. Available from: <https://doi.org/10.1371/journal.pone.0178981>. doi:10.1371/journal.pone.0178981.
- [15] Sanjabi S, Oh SA, Li MO. Regulation of the Immune Response by TGF- β : From Conception to Autoimmunity and Infection. *Cold Spring Harb Perspect Biol.* 2017 Jun;9(6).
- [16] Mina SG, Wang W, Cao Q, Huang P, Murray BT, Mahler GJ. Shear stress magnitude and transforming growth factor-Beta 1 regulate endothelial to mesenchymal transformation in a three-dimensional culture microfluidic device. *RSC Adv.* 2016;6:85457–85467. Available from: <http://dx.doi.org/10.1039/C6RA16607E>. doi:10.1039/C6RA16607E.
- [17] Wang JHC, Thampatty BP, Lin JS, Im HJ. Mechanoregulation of gene expression in fibroblasts. *Gene.* 2007 Jan;391(1-2):1–15.
- [18] Novak CM, Horst EN, Taylor CC, Liu CZ, Mehta G. Fluid shear stress stimulates breast cancer cells to display invasive and chemoresistant phenotypes while upregulating PLAU in a 3D bioreactor. *Biotechnol Bioeng.* 2019 Aug;116(11):3084–3097.
- [19] Shemesh J, Jalilian I, Shi A, Heng Yeoh G, Knothe Tate ML, Ebrahimi Warkiani M. Flow-induced stress on adherent cells in microfluidic devices. *Lab Chip.* 2015;15:4114–4127. Available from: <http://dx.doi.org/10.1039/C5LC00633C>. doi:10.1039/C5LC00633C.
- [20] Song S, Han H, Ko UH, Kim J, Shin JH. Collaborative effects of electric field and fluid shear stress on fibroblast migration. *Lab Chip.* 2013;13:1602–1611. Available from: <http://dx.doi.org/10.1039/C3LC41240G>. doi:10.1039/C3LC41240G.
- [21] Poon C. Measuring the density and viscosity of culture media for optimized computational fluid dynamics analysis of in vitro devices. *Journal of the Mechanical Behavior of Biomedical Materials.* 2022;126:105024. Available from: <https://www.sciencedirect.com/science/article/pii/S1751616121006500>. doi:<https://doi.org/10.1016/j.jmbbm.2021.105024>.
- [22] Yuan JS, Reed A, Chen F, Stewart CN Jr. Statistical analysis of real-time PCR data. *BMC Bioinformatics.* 2006 Feb;7:85.
- [23] Lu T, Oomens L, Terstappen LWMM, Prakash J. In Vivo Detection of Circulating Cancer-Associated Fibroblasts in Breast Tumor Mouse Xenograft: Impact of Tumor Stroma and Chemotherapy. *Cancers.* 2023;15(4). Available from: <https://www.mdpi.com/2072-6694/15/4/1127>. doi:10.3390/cancers15041127.
- [24] Howard EW, Crider BJ, Updike DL, Bullen EC, Parks EE, Haaksma CJ, et al. MMP-2 expression by fibroblasts is suppressed by the myofibroblast phenotype. *Exp Cell Res.* 2012 Mar;318(13):1542–1553.